2021 43rd Annual International Conference of the
IEEE Engineering in Medicine & Biology Society (EMBC)
Oct 31 - Nov 4, 2021. Virtual Conference

Parametric fMRI analysis of videos of variable arousal levels reveals different dorsal vs ventral activation preferences between autism and controls

Daniel Agostinho, Rita Correia, Isabel Catarina Duarte, Daniela Sousa, Rodolfo Abreu, Ana Pina Rodrigues, Miguel Castelo-Branco, Marco Simões

Abstract— **Atypical sensory processing is now considered a ubiquitous feature of autism spectrum disorder (ASD) and is responsible for the atypical sensory-based behaviours seen in these individuals. Specifically, emotional arousal is a critical ASD target since it comprises emotion regulation and sensory processing, two core aspects of autism. So, in this project, we used task-based fMRI and a well-catalogued dataset of videos with variable arousal levels to characterize the sensory processing of emotional arousal content in ASD and typically developed controls. Our analysis revealed a difference in the secondary attention network where ASD individuals showed a clear yet lateralized preference to the dorsal attention network, whereas the neurotypical individuals preferred the ventral attention network.**

I. Introduction

Autism spectrum disorder (ASD) is an early-onset and life-long neurodevelopmental condition characterized by deficits in social communication and interaction and the presence of restricted and repetitive patterns of behaviour, interests and/or activities [1-2]. Effective reception, integration, and processing of sensory input enable a response to environmental signals adaptively, essential to everyday functioning and learning. However, ASD individuals demonstrate difficulties with sensory modulation resulting in atypical sensory-based behaviours. These behaviours are now considered a ubiquitous feature of ASD and are included as hyper and/or hyporesponsiveness in the most recent diagnostic criteria for ASD, reported in up to 75% of individuals [3-4]. This behavioural difference [5] correlates to abnormally low or elevated levels of autonomic and behavioural arousal [6-7].

Furthermore, atypical sensory modulation in ASD individuals is linked to elevated levels of stress and anxiety. These levels of stress and anxiety can be triggered by hyperresponsive responses to particular sensory stimuli that ultimately can result in self-injurious [8-9] or other problematic behaviours [10-11], difficulties in decision making [12], and considerable stress on family systems [13], especially in those unable to communicate their distress. Furthermore, a strong link has also been found between hyperresponsiveness and the development of specific phobias, social dysfunction, and occupational performance [14–16]. Thus, hyperresponsiveness appears as a critical prior to anxiety symptoms that must be addressed to develop tools that can help modulate sensory responsivity.

One measure of responsiveness is arousal, and one significant type of arousal in ASD individuals is emotional arousal since it comprises both responsiveness to stimuli and emotion regulation, two aspects frequently compromised in ASD [17]. In fact, some studies have linked under arousal to externalizing behavioural problems in ASD [18]. In this sense, applying neuroimaging approaches to the processing of stimuli of variable emotional arousal levels can reveal essential cues on how these processes are portrayed in ASD, as opposed to neurotypical individuals.

This paper presents the preliminary results regarding the decoding of high and low emotional arousal states in the brain in both typically developing (TD) and ASD individuals using task-based fMRI and a well-catalogued stimuli dataset of stimuli with variable arousal levels [19].

II. Methods

A. Participants

In this study participated 27 individuals, 14 with ASD and 13 typically developed controls matched by age and empathy quotient. The relevant demographic information of the participants' groups is summarized in the Table I.

Table I – Demographic description of the ASD and TD groups, including age, Full-Scale Intelligence Quotient (FSIQ), Empathy Quotient (EQ), Autism Spectrum Quotient (AQ-10) and the Autism Diagnostic Observation Schedule (ADOS) score. Each score is presented in terms of group average and standard error, in brackets. Group differences were assessed with a two-sample T-test, with p-values on the last column. Groups are matched by age and EQ.

	ASD	TD	P
N	14	13	0.34
AGE	21.58(1.36)	23.15(0.91)	<0.01
FSIQ	94.50 (2.97)	111.23 (4.30)	<0.01
EQ	38.45 (4.54)	45.62 (2.89)	0.18
AQ-10	24.17 (1.49)	15.38 (1.54)	<0.01
ADOS	1.75(0.13)	-	-

This work was supported in part by the Santander/University of Coimbra seed project BioHab.

All authors are with the Coimbra Institute for Biomedical Imaging and Translational Research (CIBIT), from the Institute of Nuclear Sciences applied to Health (ICNAS) of the University of Coimbra. D. A., A. R. C. and M. S. (email: msimoes@dei.uc.pt) are also with the Center for Informatics and Systems of the University of Coimbra (CISUC).

The authors thank the participants and their families for joining the study, as well as the patients' associations of APPDA-Viseu and Coimbra that supported the recruitment.

B. *fMRI experimental task*

The fMRI experimental task was divided into three runs. Each run was constituted by ten blocks, each containing three segments: fixation cross, video, and finally patient evaluation (Fig 1.). The fixation cross segment is composed of a small white cross in a black background that is displayed during at least 15 seconds and was used as a baseline. In the video segment either a high or low arousal video form the CAAV dataset [19] was displayed. Each video has a duration of 15 seconds and comprised an interaction between two actors, viewed from a first-person perspective (e.g., hugging a person, stealing money). The emotional arousal of each video of the dataset have been catalogued by 400 participants, and these values are available along with the videos. At the end of each video, an evaluation segment is presented where the participant was asked to self-evaluate the previous video in relation to its valence and emotional arousal, using the 9-point Self-Assessment Manikin (SAM) scale.

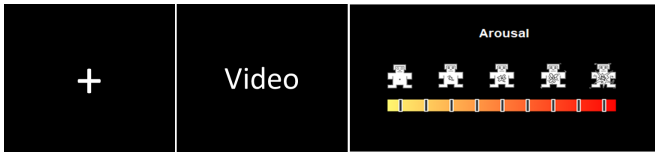

Figure 1. Illustration of the design of each run block showing the different segments that are part of it.

C. *fMRI acquisition protocol*

Imaging was performed on a 3T Siemens MAGNETOM Prisma Fit MRI scanner (Siemens, Erlangen) using a 64-channel RF receive coil, at the Portuguese Brain Imaging Network (Coimbra, Portugal). fMRI data were acquired using a 2D simultaneous multi-slice (SMS) gradient-echo echoplanar imaging (GE-EPI) sequence (6× SMS and 2× in-plane GRAPPA accelerations), with the following parameters: TR/TE = 1000/37 ms, voxel size = 2.0×2.0×2.0 mm3, 72 axial slices (whole-brain coverage), FOV = 200×200 mm2, FA = 68°, and phase encoding in the anterior-posterior direction. A short EPI acquisition (10 volumes) with reversed phase encoding direction was also performed prior to each fMRI run, for image distortion correction. A 3D anatomical T1-weighted MP2RAGE (TR = 5000 ms, TE = 3.11 ms; 192 interleaved slices with isotropic voxel size of 1 mm) was also collected for subsequent image registration.

D. *fMRI pre-processing*

Before starting the pre-processing, data from all three runs were merged using FSL's utility *fsl_merge. The merged d*ata were then pre-processed using FSL [20] according to the following pipeline. First, slice timing and motion correction were performed using FSL utility *fsl_slicetimer* and tool MCFLIRT [21] respectively. Subsequently, a B0-unwarping step was performed with FSL tool TOPUP [22], using the reversed-phase encoding acquisition, to reduce EPI distortions, followed by the correction for the bias field using FSL tools FAST [23]. Following these steps, non-brain tissue was removed using FSL tool BET [24] and nuisance fluctuations were then removed by linear regression using the following regressors [25]: 1) quasi-periodic BOLD fluctuations related to cardiac and respiratory cycles were modelled by a fourth order Fourier series using RETROICOR extracted using the PhysIO [26], 2) aperiodic BOLD fluctuations associated with changes in the heart rate as well as in the depth and rate of respiration were modelled by convolution with the respective impulse response functions also extracted using PhysIO [27], 3) the average BOLD fluctuations measured in white matter (WM) and cerebrospinal fluid (CSF) masks (obtained as described below), 4) the six motion parameters estimated by MCFLIRT, and 5) scan nulling regressors (motion scrubbing) associated with volumes acquired during periods of large head motion which were determined using the FSL utility *fsl_motion_outliers.* Finally, a high-pass temporal filtering with a cut-off period of 100 seconds was applied, and spatial smoothing using a Gaussian kernel with full width at half-maximum (FWHM) of 3 mm was performed.

E. *Structural MRI pre-processing*

For each participant, WM and CSF masks were obtained from the respective T1-weighted structural image by segmentation into grey matter (GM), WM and CSF using FSL tool FAST [22]. The functional images were then co-registered with the respective T1-weighted structural images using FSL's tool FLIRT, and subsequently with the Montreal Neurological Institute (MNI) [26] template, using FSL's toll FNIRT [20]. Both WM and CSF masks were transformed into the functional space and were then eroded using a 3 mm spherical kernel to minimize partial volume effects [27].

F. *Data analysis*

Following pre-processing, the fMRI data were analysed at two levels. First, each participant's data were analysed individually and then group analysis was performed using the FSL tool Feat [29-30]. Feat analysis is based on general linear modelling (GLM). For the first-level analysis (individual analysis), three explanatory variables (EVs) were considered corresponding to the different segments in the task protocol: 1) videos, obtained by combining all the video segments into a single regressor; 2) responses, corresponding to the response segments; and 3) fixation cross, corresponding to the fixation cross-segment. Each EV was modelled using a boxcar function and contained the information for when the event starts, its duration and its intensity. For the EV that corresponds to the combined video segments, the intensity of each event was modulated using the participants' self-evaluated arousal level, normalised intra-participant-wise to the highest reported value. Each EV was then convoluted with the double-gamma HRF function, and the BOLD signal from each voxel of the data is fitted to them. The parametric modulation of the boxcar function for the videos EV will allow to look for voxels where the BOLD signal is modulated by the arousal levels reported by the participants on a trial-by-trial basis. The resulting estimated parameters of each voxel are then stored for each EV. These parameters can be used for statistical analysis by constructing contrasts, defined in FSL as a contrast of parameter estimate (COPE), revealing activations maps related to a specific EV or a combination of EVs. For the first-level analysis, two COPEs were considered: 1) video, revealing brain regions solely involved with the first EV (videos); and 2) video vs fixation cross, revealing the brain regions that show greater activation when in the video's

segments than in the fixation cross segments. Finally, in the second-level analysis, we evaluated the mean activation across each group for all the first-level COPEs and the group difference.

III. Results

Behavioural analysis was performed to confirm the match between the values reported by the participants and the labelling from the database [19] regarding the arousal level of the videos shown. Using the Pearson correlation, the results showed that the group averages of emotional arousal values reported by the participants for each video type were highly correlated ($r \geq 0.9$) with the catalogued arousal level from the database [19] in both groups (Fig 2).

Regarding the fMRI data second-level analysis, we observe differences in activation patterns between the two groups (Fig 3). It is possible to identify that the ASD group shows greater activation of the dorsal attention network (DAN), with higher recruitment of the intraparietal sulcus (IPS). In contrast, the TD group shows greater activation of the ventral attention network (VAN), especially in regions from the temporoparietal junction (TPJ) complex. Furthermore, we observe a right-lateralization of the activation for the ASD group. This right-lateralization is well documented regarding emotional responses [31] and alterations to such lateralization have also been associated with sensory disorders and deficits [32].

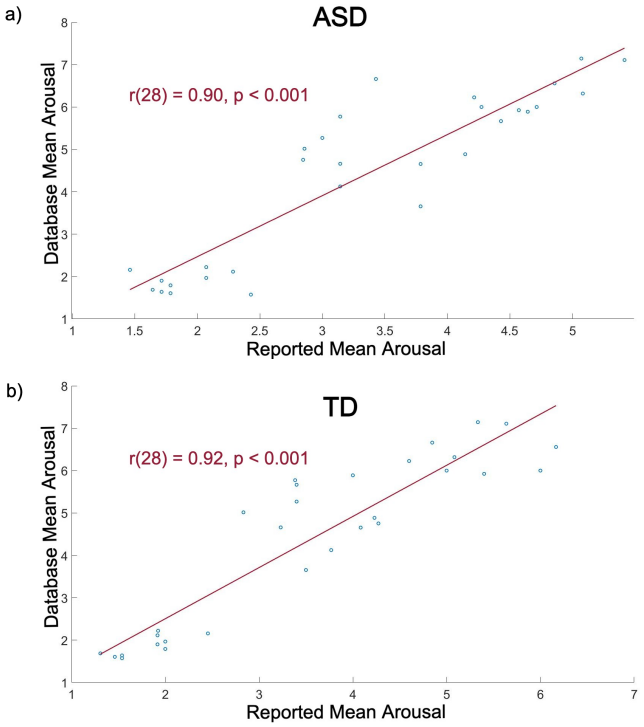

Figure 2. Results from the behavioural analysis. It is possible to see that in both the Clinical a) and Control b) groups there is a high correlation between the answer given by the participant and the expected value from the database [19].

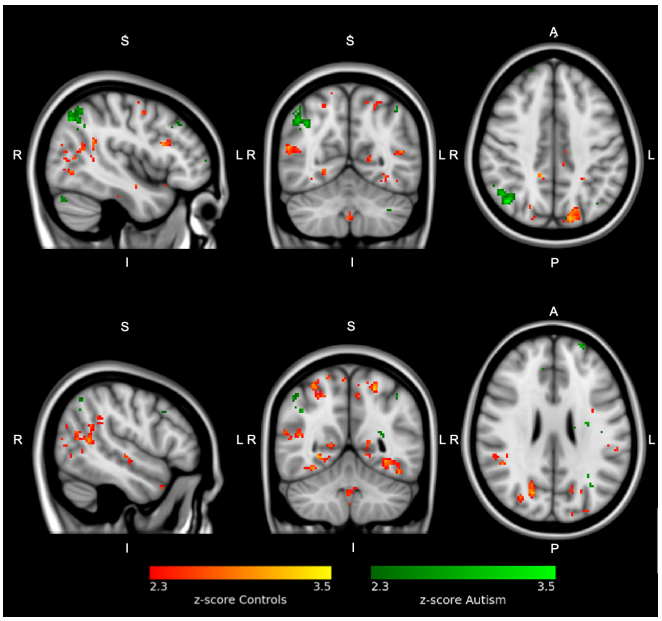

Figure 3. Maps of z-score activation for the voxels that show significant difference in activation between the two groups. In red, voxels where the activation is greater in the Control group, and in green voxels where the activation is greater in the Autism group. Slices from a) (x:44, y:-60, z:42), b) (x:51, y: -54, z:26) in the MNI space.

IV. Discussion

The results from the fMRI analysis showed an interesting difference regarding how the events, in this case, videos of variable emotional arousal content, are processed in neurotypical brains and in ASD. The results show that ASD patients make preferential use of the DAN when processing those stimuli. The DAN is a secondary attention system that is active when attention is overtly or covertly oriented in space. DAN processing focuses upon egocentric space, that is, knowing the location of observed objects in relation to the self, to generate sensory-motor information about how to interact with the object being observed. Furthermore, DAN is involved in the selection of the appropriate response or action necessary for the attention orientation [33-35]. In contrast, the TD group shows a preference for the VAN. The VAN is also a secondary attention system that is linked to directing attention to salient sensory events. The VAN then redirects the attention network towards behaviourally relevant stimuli, especially when these stimuli are initially unattended. Furthermore, the focus of the VAN is focused primarily upon allocentric space, that is, knowing the relative location of objects in relation to other objects [33-34].

This difference in the activation of the different secondary attention systems reveals a fundamental difference in how the ASD participants process sensory information regarding the interaction of other persons, focusing more on the spatial identification of the scenery and how they can interact with it rather than analysing the interaction between the participants in the action and processing the sensory information observer from their interaction.

Furthermore, the over recruitment of the right parietal area by the ASD group is consistent with our previous works on emotion perception and imagination [36].

Our results corroborate the differences reported in the literature in terms of emotional arousal responses when compared to TD individuals, providing new insights regarding the attentional aspects of sensory processing of stimuli with emotional arousal content. The differences here identified highlight the need for tailored interventions for emotional regulation in autism.

REFERENCES

[1] J. Hyde and E. Garcia-Rill, Autism and arousal. Elsevier Inc., 2019.

[2] E. J. Marco, L. B. N. Hinkley, S. S. Hill, and S. S. Nagarajan, "Sensory Processing in Autism: A Review of Neurophysiologic Findings," Pediatr. Res., vol. 69, no. 5 Part 2, pp. 48R-54R, May 2011, doi: 10.1203/PDR.0b013e3182130c54.

[3] D. Green, S. Chandler, T. Charman, E. Simonoff, and G. Baird, "Brief Report: DSM-5 Sensory Behaviours in Children With and Without an Autism Spectrum Disorder," J. Autism Dev. Disord., vol. 46, no. 11, pp. 3597–3606, Nov. 2016, doi: 10.1007/s10803-016-2881-7.

[4] D. N. Top, S. G. Luke, K. G. Stephenson, and M. South, "Psychophysiological arousal and auditory sensitivity in a cross-clinical sample of autistic and non-autistic anxious adults," Front. Psychiatry, vol. 9, no. January, pp. 1–12, 2018, doi: 10.3389/fpsyt.2018.00783.

[5] M. South and J. Rodgers, "Sensory, Emotional and Cognitive Contributions to Anxiety in Autism Spectrum Disorders," Front. Hum. Neurosci., vol. 11, Jan. 2017, doi: 10.3389/fnhum.2017.00020.

[6] W. Hirstein, P. Iversen, and V. S. Ramachandran, "Autonomic responses of autistic children to people and objects," Proc. R. Soc. London. Ser. B Biol. Sci., vol. 268, no. 1479, pp. 1883–1888, Sep. 2001, doi: 10.1098/rspb.2001.1724.

[7] M. Kinsbourne, "Cerebral-Brainstem Relations in Infantile Autism," in Neurobiological Issues in Autism, Boston, MA: Springer US, 1987, pp. 107–125.

[8] T. R. Buck et al., "Psychiatric Comorbidity and Medication Use in Adults with Autism Spectrum Disorder," J. Autism Dev. Disord., vol. 44, no. 12, pp. 3063–3071, Dec. 2014, doi: 10.1007/s10803-014-2170-2.

[9] C. M. Kerns et al., "Traditional and Atypical Presentations of Anxiety in Youth with Autism Spectrum Disorder," J. Autism Dev. Disord., vol. 44, no. 11, pp. 2851–2861, Nov. 2014, doi: 10.1007/s10803-014-2141-7.

[10] K. Gotham et al., "Exploring the Relationship Between Anxiety and Insistence on Sameness in Autism Spectrum Disorders," Autism Res., vol. 6, no. 1, pp. 33–41, Feb. 2013, doi: 10.1002/aur.1263.

[11] J. Rodgers, M. Glod, B. Connolly, and H. McConachie, "The Relationship Between Anxiety and Repetitive Behaviours in Autism Spectrum Disorder," J. Autism Dev. Disord., vol. 42, no. 11, pp. 2404–2409, Nov. 2012, doi: 10.1007/s10803-012-1531-y.

[12] L. Luke, I. C. H. Clare, H. Ring, M. Redley, and P. Watson, "Decision-making difficulties experienced by adults with autism spectrum conditions," Autism, vol. 16, no. 6, pp. 612–621, Nov. 2012, doi: 10.1177/1362361311415876.

[13] C. M. Conner, B. B. Maddox, and S. W. White, "Parents' State and Trait Anxiety: Relationships with Anxiety Severity and Treatment Response in Adolescents with Autism Spectrum Disorders," J. Autism Dev. Disord., vol. 43, no. 8, pp. 1811–1818, Aug. 2013, doi: 10.1007/s10803-012-1728-0.

[14] A. Muskett, S. Radtke, S. White, and T. Ollendick, "Autism Spectrum Disorder and Specific Phobia: the Role of Sensory Sensitivity: Brief Review," Rev. J. Autism Dev. Disord., vol. 6, no. 3, pp. 289–293, 2019, doi: 10.1007/s40489-019-00159-w.

[15] K. Roelofs, J. van Peer, E. Berretty, P. de Jong, P. Spinhoven, and B. M. Elzinga, "Hypothalamus–Pituitary–Adrenal Axis Hyperresponsiveness Is Associated with Increased Social Avoidance Behavior in Social Phobia," Biol. Psychiatry, vol. 65, no. 4, pp. 336–343, Feb. 2009, doi: 10.1016/j.biopsych.2008.08.022.

[16] B. Kashefimehr, H. Kayihan, and M. Huri, "The effect of sensory integration therapy on occupational performance in children with autism," OTJR Occup. Particip. Heal., vol. 38, no. 2, pp. 75–83, 2018, doi: 10.1177/1539449217743456.

[17] Zantinge, G., van Rijn, S., Stockmann, L. et al. Physiological Arousal and Emotion Regulation Strategies in Young Children with Autism Spectrum Disorders. J Autism Dev Disord 47, 2648–2657 (2017). https://doi.org/10.1007/s10803-017-3181-6

[18] Baker JK, Fenning RM, Erath SA, Baucom BR, Moffitt J, Howland MA. Sympathetic Under-Arousal and Externalizing Behavior Problems in Children with Autism Spectrum Disorder. J Abnorm Child Psychol. 2018;46(4):895-906. doi:10.1007/s10802-017-0332-3

[19] A. Di Crosta et al., "The Chieti Affective Action Videos database, a resource for the study of emotions in psychology," Sci. Data, vol. 7, no. 1, pp. 1–6, 2020, doi: 10.1038/s41597-020-0366-1.

[20] M. W. Woolrich et al., "Bayesian analysis of neuroimaging data in FSL," Neuroimage, vol. 45, no. 1, pp. S173–S186, Mar. 2009, doi: 10.1016/j.neuroimage.2008.10.055.

[21] M. Jenkinson, "Improved Optimization for the Robust and Accurate Linear Registration and Motion Correction of Brain Images," Neuroimage, vol. 17, no. 2, pp. 825–841, Oct. 2002, doi: 10.1016/S1053-8119(02)91132-8.

[22] J. L. R. Andersson, S. Skare, and J. Ashburner, "How to correct susceptibility distortions in spin-echo echo-planar images: application to diffusion tensor imaging," Neuroimage, vol. 20, no. 2, pp. 870–888, Oct. 2003, doi: 10.1016/S1053-8119(03)00336-7.

[23] Y. Zhang, M. Brady, and S. Smith, "Segmentation of brain MR images through a hidden Markov random field model and the expectation-maximization algorithm," IEEE Trans. Med. Imaging, vol. 20, no. 1, pp. 45–57, 2001, doi: 10.1109/42.906424.

[24] M. Jenkinson, M. Pechaud, and S. Smith. BET2: MR-based estimation of brain, skull and scalp surfaces. In Eleventh Annual Meeting of the Organization for Human Brain Mapping, 2005.

[25] R. Abreu, S. Nunes, A. Leal, and P. Figueiredo, "Physiological noise correction using ECG-derived respiratory signals for enhanced mapping of spontaneous neuronal activity with simultaneous EEG-fMRI," Neuroimage, vol. 154, pp. 115–127, Jul. 2017, doi: 10.1016/j.neuroimage.2016.08.008.

[26] L. Kasper et al., "The PhysIO Toolbox for Modeling Physiological Noise in fMRI Data," J. Neurosci. Methods, vol. 276, pp. 56–72, Jan. 2017, doi: 10.1016/j.jneumeth.2016.10.019.

[27] D. L. Collins, P. Neelin, T. M. Peters, and A. C. Evans, "Automatic 3D Intersubject Registration of MR Volumetric Data in Standardized Talairach Space," J. Comput. Assist. Tomogr., vol. 18, no. 2, pp. 192–205, Mar. 1994, doi: 10.1097/00004728-199403000-00005

[28] H. J. Jo, Z. S. Saad, W. K. Simmons, L. A. Milbury, and R. W. Cox, "Mapping sources of correlation in resting state FMRI, with artifact detection and removal," Neuroimage, vol. 52, no. 2, pp. 571–582, Aug. 2010, doi: 10.1016/j.neuroimage.2010.04.246.

[29] M. W. Woolrich, T. E. J. Behrens, and S. M. Smith, "Constrained linear basis sets for HRF modelling using Variational Bayes," Neuroimage, vol. 21, no. 4, pp. 1748–1761, Apr. 2004, doi: 10.1016/j.neuroimage.2003.12.024.

[30] M. W. Woolrich, T. E. J. Behrens, C. F. Beckmann, M. Jenkinson, and S. M. Smith, "Multilevel linear modelling for FMRI group analysis using Bayesian inference," Neuroimage, vol. 21, no. 4, pp. 1732–1747, Apr. 2004, doi: 10.1016/j.neuroimage.2003.12.023.

[31] Guido Gainotti. 2019. Emotions and the Right Hemisphere: Can New Data Clarify Old Models? Neuroscientist 25, 3: 258–270. https://doi.org/10.1177/1073858418785342

[32] Giulia Cartocci, Andrea Giorgi, Bianca M.S. Inguscio, Alessandro Scorpecci, Sara Giannantonio, Antonietta De Lucia, Sabina Garofalo, Rosa Grassia, Carlo Antonio Leone, Patrizia Longo, Francesco Freni, Paolo Malerba, and Fabio Babiloni. 2021. Higher Right Hemisphere Gamma Band Lateralization and Suggestion of a Sensitive Period for Vocal Auditory Emotional Stimuli Recognition in Unilateral Cochlear Implant Children: An EEG Study. Frontiers in Neuroscience 15, March: 1–10. https://doi.org/10.3389/fnins.2021.608156

[33] S. Vossel, J. J. Geng, and G. R. Fink, "Dorsal and Ventral Attention Systems," Neurosci., vol. 20, no. 2, pp. 150–159, Apr. 2014, doi: 10.1177/1073858413494269.

[34] M. D. Fox, M. Corbetta, A. Z. Snyder, J. L. Vincent, and M. E. Raichle, "Spontaneous neuronal activity distinguishes human dorsal and ventral attention systems," Proc. Natl. Acad. Sci., vol. 103, no. 26, pp. 10046–10051, Jun. 2006, doi: 10.1073/pnas.0604187103.

[35] S. Caspers, K. Amunts, and K. Zilles, "Posterior Parietal Cortex," in The Human Nervous System, Elsevier, 2012, pp. 1036–1055.

[36] Simões, M., Monteiro, R., Andrade, J., Mouga, S., França, F., Oliveira, G., Carvalho, P., & Castelo-Branco, M. (2018). A Novel Biomarker of Compensatory Recruitment of Face Emotional Imagery Networks in Autism Spectrum Disorder. Frontiers in Neuroscience, 12(NOV), 1–15. https://doi.org/10.3389/fnins.2018.00791